STATISTICS, OPTIMIZATION AND INFORMATION COMPUTING
Stat., Optim. Inf. Comput., Vol. **15**, March 2026, pp 1554–1575.
Published online in International Academic Press (www.IAPress.org)

Bayesian Estimation, Bayesian Neural Network and Maximum Likelihood Estimation for a Novel Transmuted Tangent Family of Distributions with Applications in Healthcare Data

Amrutha P T, Rajitha C S*

Department of Mathematics, Amrita School of Physical Sciences, Coimbatore, Amrita Vishwa Vidyapeetham, India

Abstract Cancer is currently the main cause of primary or secondary premature mortality in most countries. Medical researchers require statistical analysis to identify the most suitable model for assessing the remission periods or survival times of cancer patients, thereby producing precise results. The current study contributes a novel family of distributions to analyse the remission periods or survival times of cancer data effectively, termed the transmuted tangent family of distributions, achieved through the combination of the quadratic transmuted family with the tan-G class of distributions. The primary statistical properties of the proposed family are established. The Bayesian estimation, Bayesian neural network, and maximum likelihood estimation methods are employed for parametric estimation of the family. In addition, four members of the family are introduced. The transmuted tangent Lindley distribution is examined, and its fundamental features are established. Three cancer datasets are examined to verify the fit efficiency of the proposed family through the use of various goodness-of-fit measures. Our results indicate that the proposed family offers a better fit to the data sets compared to many established families.

Keywords Bayesian estimation, Bayesian neural network, Cancer data analysis, Transmuted family, Tan-G class of distributions.

AMS 2010 subject classifications 62F40,62G05,62N02,62P10

DOI: 10.19139/soic-2310-5070-2959

1. Introduction

Cancer is presently the primary or secondary leading cause of premature mortality in the majority of countries all over the world. The worldwide incidence of cancer patients is expected to increase over the next 50 years due to significant demographic changes, including population aging and growth, which affect the varying trends in cancer incidence across different regions. The cancer incidence is projected to double by 2070 relative to 2020 [37]. Statistical distributions play a vital role in predicting and analysing the remission periods or survival times of cancer patients. Although classical distributions are versatile, they often struggle to effectively fit complex or highly skewed data sets. Their inherent structure may not display critical data characteristics such as heavy tails, multi-modality, etc. Due to the greater applicability and predictability of the distributions, researchers have begun to develop more flexible and accurate distributions to model different data sets from different fields. The most popular method to increase the flexibility of the existing distribution is to add parameters to the distribution, which leads to a greater number of parameters. Also, obtaining the parameter estimates of these flexible probability distributions with a larger number of parameters may be challenging using numerical methods. The main objective of this study is to introduce a family to generate distributions with fewer parameters and enhanced flexibility. Moreover, one of the strong members of the family is introduced, which possesses superior analytical ability towards the cancer data.

*Correspondence to: Rajitha C S (Email: cs_rajitha@cb.amrita.edu, rajitha.sugun@gmail.com).

ISSN 2310-5070 (online) ISSN 2311-004X (print)

There are many generalised families available in the literature. For example, the transformed transformer family by Alzaatreh et al. [4], power Lindley-G family of distributions by Hassan and Nassr [11], the generalised Topp-Leone family of distributions by Mahdavi and Abbas [21], Marshall-Olkin family by Marshall and Olkin [24] etc.
The number of probability distributions based on trigonometric functions is limited in the literature. Some of them are the sine-G class of distributions by Souza et al. [38], transmuted sine-G Family of distributions by Sakthivel and Rajkumar [34], hyperbolic cosine-F-family of distributions by Kharazmi and Saadatinik [15], odd hyperbolic cosine-FG family by Kharazmi et al. [16], a new sine-G family of distributions by Mahmood et al. [22], the hyperbolic tan-X family of distributions by Ampadu [5], hyperbolic tangent family of distributions by Mohammad and Mendoza [26] etc.

In 1958, Jowett [13] introduced the exponential distribution (ED) and its applications. The ED was frequently utilised for analysing real data in the initial phases of reliability theory research because of its analytical simplicity. In the present scenario, the constant failure rate characteristic of the ED is often unsuitable. The power unit ED is introduced by Alsadat et al. [3]. Lindley [19] proposed the Lindley (L) distribution as an alternative to the ED, which has an increasing failure rate. The L distribution provides a unimodal hazard rate, which increases modelling flexibility, making it a theoretically strong and often empirically effective baseline for estimating survival times in diverse health and reliability research. There are numerous generalisations for the L distribution, the odd Weibull L distribution by Rajitha and Anisha [30], the generalisation of the L distribution by Rajitha and Akhilnath [29], and a new generalisation of the power L distribution by Rajitha and Sakthivel [10]. Additional comparable generalised distributions can be found in [35], [31], [14], [27] and [32].

The estimation of the parameters of the distributions is not always easy. In the era of artificial intelligence and deep learning, it is crucial to find alternatives to classical estimation methods. In this article, three different estimation methods are used, that is, the Bayesian estimation method, Bayesian neural network (BNN) [25], and maximum likelihood estimation (MLE). Bayesian estimation is an effective method for parameter estimation. The Bayesian estimation of the parameters of the generalised L distribution using a trigonometric transformation is presented in [12], while Makhdoom et.al [23] discusses estimation of the parameters of the L distribution under a Type-II censoring scheme using Bayesian inference. The parameter estimation of the pseudo-L distribution using the Bayesian estimation is done in [8]. The Bayesian estimation of power L distribution based on progressively censored samples is described in [17].
The neural network and its related areas are growing rapidly. The application of neural networks in data analysis is studied in [41]. Neal [28] illustrates how Bayesian methods enable the utilisation of complex neural network models while decreasing the risk of ”overfitting” associated with conventional training methods, and the recent approaches in BNN are discussed in [20]. The robustness of the BNN to adversarial attacks is studied by Bortolussi et al. [6].

The objective of this paper is to present a superior and novel model that is adept at modeling and fitting various data types. Additionally, we aim to demonstrate the model's superiority over its competitors and endorse the proposed family of distributions as a robust and innovative candidate for modelling real data sets. When modeling a phenomenon with a known distribution proves difficult, we may employ generalization to accommodate additional data variability. The existing challenges are evolving noticeably in parallel with our needs. Consequently, we necessitate alternative generalizations of probability distributions to encapsulate complex data. As the number of cancer patients increases in almost every country, we attempted to model these data using generalized forms of various distributions; nevertheless, the results were not especially convincing. Consequently, we propose a novel family of distributions to address this issue. The motivation of this article is to introduce a novel family that is capable of generalizing existing distributions to enhance the flexibility of the distributions. This novel family adds only one parameter to the existing distributions. Adding more parameters may increase flexibility, but it also makes the estimation and calculation of the parameters more complex. The proposed family can be used to model medical data, as medical researchers require statistical analysis to evaluate survival rates of cancer patients to select the most precise model to estimate survival data and reach appropriate conclusions. The structure of the article is as follows: Section 2 presents the transmuted tangent family of distributions (TTFD), and in Section 3, the main statistical properties of the TTFD are derived. Section 4 provides the four special members of the family, in particular the transmuted tangent Lindley distribution (TTLD). The parameters of the TTLD are estimated using three different methods. Data analysis using three sets of cancer data is carried out in Section 5. The results are delineated in Section 6. The conclusion of this study is provided in Section 7.

2. Transmuted tangent family

This paper contributes a new family to the trigonometric family of distributions by combining the quadratic transmuted family with the tan-G class of distributions. The quadratic rank transmutation map approach is introduced by Shaw and Buckley [36] and its cumulative distribution function (cdf) and probability density function (pdf) are given, respectively, as follows,

$$F(x) = (1+\beta)W(x) - \beta W^2(x), |\beta| \leq 1. \tag{1}$$

$$f(x) = w(x)[(1+\beta) - 2\beta W(x)], |\beta| \leq 1. \tag{2}$$

where $W(x)$ is the cdf and $w(x)$ is the pdf of the baseline distribution.

The tan-G class of distributions is introduced by Souza et al. [40], and its cdf is given by

$$W(x) = \tan(\frac{\pi}{4}G(x)), x \in \mathbb{R}. \tag{3}$$

The pdf of the tan-G class of distributions is given by

$$w(x) = \frac{\pi}{4}g(x)\sec^2(\frac{\pi}{4}G(x)), x \in \mathbb{R}. \tag{4}$$

The TTFD, achieved through the combination of the quadratic transmuted family with the tan-G class of distributions; then the cdf of the TTFD is derived as

$$F(x) = (1+\beta)\tan\left[\frac{\pi}{4}G(x)\right] - \beta\left(\tan\left[\frac{\pi}{4}G(x)\right]\right)^2, |\beta| \leq 1, x \in \mathbb{R}. \tag{5}$$

The pdf of the TTFD is derived as

$$f(x) = \frac{\pi}{4}g(x)\sec^2\left[\frac{\pi}{4}G(x)\right]\left((1+\beta) - 2\beta\tan\left[\frac{\pi}{4}G(x)\right]\right), |\beta| \leq 1, x \in \mathbb{R}. \tag{6}$$

where $G(x)$ is the cdf and $g(x)$ is the pdf of the baseline distribution.

3. Properties

This section provides the important properties of TTFD.

3.1. Survival function

The survival function (SF) for the TTFD is obtained as

$$R(x) = 1 - \left[(1+\beta)\tan\left[\frac{\pi}{4}G(x)\right] - \beta\left(\tan\left[\frac{\pi}{4}G(x)\right]\right)^2\right], |\beta| \leq 1, x \in \mathbb{R}. \tag{7}$$

The SF quantifies the ability of a product or object to survive over a specified time frame under all conditions.

3.2. Hazard function

The hazard function (HF) is the ratio of $f(x)$ and $R(x)$, which gives an idea about the instantaneous failure rate of the item at time x. The HF of the TTFD is derived as,

$$H(x) = \frac{\frac{\pi}{4}\sec^2\left[\frac{\pi}{4}G(x)\right]g(x)\left((1+\beta) - 2\beta\tan\left[\frac{\pi}{4}G(x)\right]\right)}{1 - \left[(1+\beta)\tan\left[\frac{\pi}{4}G(x)\right] - \beta(\tan\left[\frac{\pi}{4}G(x)\right])^2\right]}, |\beta| \leq 1, x \in \mathbb{R}. \tag{8}$$

3.3. *Reverse hazard function*

The reverse hazard function of the TTFD is obtained as

$$r(x) = \frac{\frac{\pi}{4}\sec^2\left[\frac{\pi}{4}G(x)\right]g(x)\left((1+\beta)-2\beta\tan\left[\frac{\pi}{4}G(x)\right]\right)}{(1+\beta)\tan\left[\frac{\pi}{4}G(x)\right]-\beta(\tan\left[\frac{\pi}{4}G(x)\right])^2}, |\beta| \leq 1, x \in \mathbb{R}. \tag{9}$$

3.4. *Moments*

The main properties of a distribution can be studied through the examination of moments. The m^{th} moment of the TTFD is obtained as

$$\mu'_m = E(x_m) = \frac{\pi}{4}\int_{-\infty}^{\infty} x^m g(x)\sec^2\left[\frac{\pi}{4}G(x)\right]\left((1+\beta)-2\beta\tan\left[\frac{\pi}{4}G(x)\right]\right)dx. \tag{10}$$

where $m = 1, 2, 3, \cdots$. By finding the solution of the above equation, we get the moments of the TTFD.

3.5. *Order statistics*

The pdf of the i^{th} order statistic derived for a random sample of size m drawn from the TTFD with cdf eqn.(5) and pdf eqn.(6) is denoted by $f_i(x)$. Let the order statistics are $x_{1:m} \leq x_{2:m} \leq x_{3:m} \leq \cdots \leq x_{m:m}$. The pdf of the i^{th} order statistics of the TTFD is obtained as

$$f_i(x) = \left\{\begin{array}{l} \frac{m!}{(i-1)!(m-i)!}\left[(1+\beta)\tan\left[\frac{\pi}{4}G(x)\right]-\beta\left(\tan\left[\frac{\pi}{4}G(x)\right]\right)^2\right]^{i-1} \\ \times\left[1-(1+\beta)\tan\left[\frac{\pi}{4}G(x)\right]-\beta\left(\tan\left[\frac{\pi}{4}G(x)\right]\right)^2\right]^{m-i} \\ \times\frac{\pi}{4}g(x)\sec^2\left[\frac{\pi}{4}G(x)\right]\left((1+\beta)-2\beta\tan\left[\frac{\pi}{4}G(x)\right]\right), \\ \hfill |\beta| \leq 1, x \in \mathbb{R}. \end{array}\right\} \tag{11}$$

The first-order statistic of the TTFD is obtained as

$$f_1(x) = \left\{\begin{array}{l} m\left[1-(1+\beta)\tan\left[\frac{\pi}{4}G(x)\right]-\beta\left(\tan\left[\frac{\pi}{4}G(x)\right]\right)^2\right]^{m-1} \\ \times\frac{\pi}{4}g(x)\sec^2\left[\frac{\pi}{4}G(x)\right]\left((1+\beta)-2\beta\tan\left[\frac{\pi}{4}G(x)\right]\right), \\ \hfill |\beta| \leq 1, x \in \mathbb{R}. \end{array}\right\}$$

The m^{th} order statistics of the TTFD is obtained as

$$f_m(x) = \left\{\begin{array}{l} m\left[(1+\beta)\tan\left[\frac{\pi}{4}G(x)\right]-\beta\left(\tan\left[\frac{\pi}{4}G(x)\right]\right)^2\right]^{m-1} \\ \times\frac{\pi}{4}g(x)\sec^2\left[\frac{\pi}{4}G(x)\right]\left((1+\beta)-2\beta\tan\left[\frac{\pi}{4}G(x)\right]\right), \\ \hfill |\beta| \leq 1, x \in \mathbb{R}. \end{array}\right\}$$

3.6. *Quantile function*

The quantile function is the inverse of the cdf and it plays a crucial role in statistical analysis, as it facilitates random number generation.

Theorem 3.1
Consider the random variable X from the TTFD; then the quantile function of X is derived as

$$Q_x(p) = G^{-1}\left[\frac{4}{\pi}\arctan\left(\frac{(1+\beta)\pm\sqrt{(1+\beta)^2-4\beta p}}{2\beta}\right)\right], |\beta| \leq 1. \tag{12}$$

Proof
The quantile function of the TTFD is obtained by equating the $F(x) = p$, where $p \in (0, 1)$.

$$(1+\beta)\tan\left[\frac{\pi}{4}G(x)\right] - \beta\left(\tan\left[\frac{\pi}{4}G(x)\right]\right)^2 = p.$$

$$\tan\left[\frac{\pi}{4}G(x)\right] = \left(\frac{(1+\beta)\pm\sqrt{(1+\beta)^2-4\beta p}}{2\beta}\right).$$

$$\frac{\pi}{4}G(x) = \arctan\left(\frac{(1+\beta)\pm\sqrt{(1+\beta)^2-4\beta p}}{2\beta}\right).$$

After some simple mathematical calculations, the quantile function is obtained as

$$Q_x(p) = G^{-1}\left[\frac{4}{\pi}\arctan\left(\frac{(1+\beta)\pm\sqrt{(1+\beta)^2-4\beta p}}{2\beta}\right)\right], |\beta| \leq 1.$$

The plus or minus sign in the Eq.(12) depends on the range of the baseline distribution. □

3.7. Parameter identifiability

The parameter identification of the TTFD is proved in this section. Let β_1 and β_2 are parameters of the TTFD and δ_1 and δ_2 are the parameters of the baseline distribution of the TTFD with cdf's

$$F(x, \beta_1, \delta_1) = (1+\beta_1)\tan\left[\frac{\pi}{4}G(x,\delta_1)\right] - \beta_1\left(\tan\left[\frac{\pi}{4}G(x,\delta_1)\right]\right)^2.$$

and

$$F(x, \beta_2, \delta_2) = (1+\beta_2)\tan\left[\frac{\pi}{4}G(x,\delta_2)\right] - \beta_2\left(\tan\left[\frac{\pi}{4}G(x,\delta_2)\right]\right)^2.$$

The parameters are said to be identifiable if $F(x, \beta_1, \delta_1) = F(x, \beta_2, \delta_2)$ it implies $\beta_1 = \beta_2$ and $\delta_1 = \delta_2$. If

$$(1+\beta_1)\tan\left[\frac{\pi}{4}G(x,\delta_1)\right] - \beta_1\left(\tan\left[\frac{\pi}{4}G(x,\delta_1)\right]\right)^2 = (1+\beta_2)\tan\left[\frac{\pi}{4}G(x,\delta_2)\right] - \beta_2\left(\tan\left[\frac{\pi}{4}G(x,\delta_2)\right]\right)^2.$$

The above equation can be simplified as

$$\tan\left[\frac{\pi}{4}G(x,\delta_1)\right] + \beta_1\left(\tan\left[\frac{\pi}{4}G(x,\delta_1)\right] - \left(\tan\left[\frac{\pi}{4}G(x,\delta_2)\right]\right)^2\right) = \tan\left[\frac{\pi}{4}G(x,\delta_2)\right] + \beta_2\left(\tan\left[\frac{\pi}{4}G(x,\delta_2)\right] - \left(\tan\left[\frac{\pi}{4}G(x,\delta_2)\right]\right)^2\right) \tag{13}$$

If $\tan\left[\frac{\pi}{4}G(x,\delta_1)\right] = \tan\left[\frac{\pi}{4}G(x,\delta_2)\right]$, by injectivity properties of the tan function and cdf function of the baseline distribution also for every x and δ the $G(x, \delta) \in (0, 1)$, which implies $\delta_1 = \delta_2$. Then the eqn(13) can be written as

$$\beta_1\left(\tan\left[\frac{\pi}{4}G(x,\delta)\right] - \left(\tan\left[\frac{\pi}{4}G(x,\delta)\right]\right)^2\right) = \beta_2\left(\tan\left[\frac{\pi}{4}G(x,\delta)\right] - \left(\tan\left[\frac{\pi}{4}G(x,\delta)\right]\right)^2\right).$$

Which implies,

$$(\beta_1 - \beta_2)\left(\tan\left[\frac{\pi}{4}G(x,\delta)\right] - \left(\tan\left[\frac{\pi}{4}G(x,\delta)\right]\right)^2\right) = 0. \tag{14}$$

The left-hand side of the eqn(14) is zero when $\beta_1 = \beta_2$.

4. Special models of TTFD

This section presents four unique members of the TTFD by choosing different baseline distributions.The exponential distribution, Weibull distribution, Rayleigh distribution, and Lindley distribution are selected as the baseline distributions because all the distributions possess good modelling properties for survival data. We can also generalise all other distributions using TTFD.

4.1. *Transmuted tangent exponential distribution*

The cdf of the ED is given by

$$G(x) = 1 - e^{-\alpha x},\ \alpha > 0, x \geq 0. \tag{15}$$

The pdf of the ED is given by

$$g(x) = \alpha e^{-\alpha x},\ \alpha > 0, x \geq 0. \tag{16}$$

The cdf of the transmuted tangent exponential distribution (TTED) is obtained as

$$F(x) = (1+\beta)\tan\left[\frac{\pi}{4}[1-e^{-\alpha x}]\right] - \beta\left(\tan\left[\frac{\pi}{4}[1-e^{-\alpha x}]\right]\right)^2, |\beta| \leq 1, \alpha > 0, x \geq 0. \tag{17}$$

The pdf of the TTED is obtained as

$$f(x) = \frac{\pi\alpha}{4}e^{-\alpha x}\sec^2\left[\frac{\pi}{4}[1-e^{-\alpha x}]\right]\left((1+\beta) - 2\beta\tan\left[\frac{\pi}{4}[1-e^{-\alpha x}]\right]\right),$$
$$|\beta| \leq 1, \alpha > 0x \geq 0. \tag{18}$$

The HF of the TTED is obtained as

$$H(x) = \frac{\frac{\pi\alpha}{4}e^{-\alpha x}\sec^2\left[\frac{\pi}{4}[1-e^{-\alpha x}]\right]\left((1+\beta) - 2\beta\tan\left[\frac{\pi}{4}[1-e^{-\alpha x}]\right]\right)}{1-(1+\beta)\tan\left[\frac{\pi}{4}[1-e^{-\alpha x}]\right] - \beta\left(\tan\left[\frac{\pi}{4}[1-e^{-\alpha x}]\right]\right)^2},$$
$$|\beta| \leq 1, \alpha > 0, x \geq 0. \tag{19}$$

The SF of the TTED is obtained as

$$R(x) = 1-(1+\beta)\tan\left[\frac{\pi}{4}[1-e^{-\alpha x}]\right] - \beta\left(\tan\left[\frac{\pi}{4}[1-e^{-\alpha x}]\right]\right)^2, |\beta| \leq 1, \alpha > 0, x \geq 0. \tag{20}$$

The plot of the cdf of the TTED is shown in Fig. 1(a). The plot of the pdf of the TTED is shown in Fig.1(b). The HF plot of TTED with different shapes, including increasing, decreasing, and J-shaped, is shown in Fig.1(c). The SF plot of TTED is shown in Fig.1(d).

4.2. *Transmuted tangent Weibull distribution*

The cdf of the Weibull distribution is given by

$$G(x) = 1 - e^{-\alpha x^{\gamma}}, \alpha, \gamma > 0, x > 0. \tag{21}$$

The pdf of the Weibull distribution is given by

$$g(x) = \alpha\gamma x^{\gamma-1}e^{-\alpha x^{\gamma}}, \alpha, \gamma > 0, x > 0. \tag{22}$$

The cdf of the transmuted tangent Weibull distribution (TTWD) is obtained as

$$F(x) = (1+\beta)\tan\left[\frac{\pi}{4}(1-e^{-\alpha x^{\gamma}})\right] - \beta\left(\tan\left[\frac{\pi}{4}(1-e^{-\alpha x^{\gamma}})\right]\right)^2, x > 0, |\beta| \leq 1, \alpha, \gamma > 0. \tag{23}$$

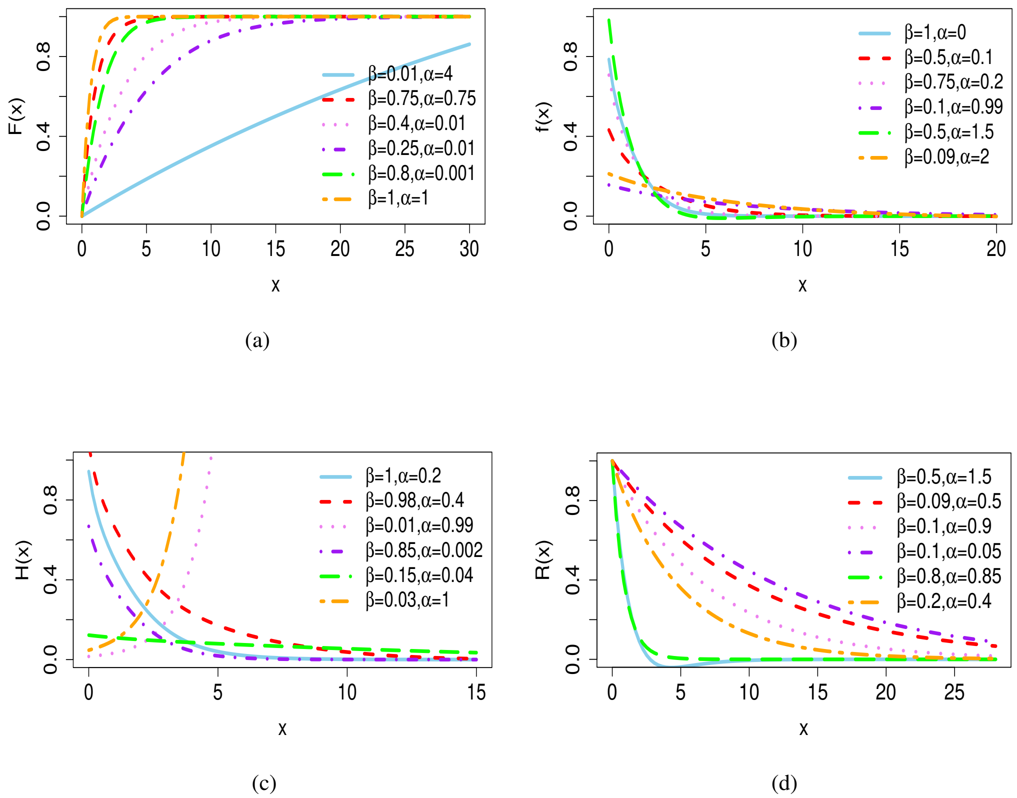

Figure 1. The cdf, pdf, HF and SF plots of the TTED.

The pdf of the TTWD is obtained as

$$f(x) = \frac{\pi}{4}\sec^2\left[\frac{\pi}{4}(1-e^{-\alpha x^\gamma})\right](\alpha\gamma x^{\gamma-1}e^{-\alpha x^\gamma})\left((1+\beta)-2\beta\tan\left[\frac{\pi}{4}(1-e^{-\alpha x^\gamma})\right]\right), \quad x>0, |\beta|\le 1, \alpha,\gamma>0. \tag{24}$$

The HF of the TTWD is obtained as

$$H(x) = \frac{\frac{\pi}{4}\sec^2\left[\frac{\pi}{4}(1-e^{-\alpha x^\gamma})\right](\alpha\gamma x^{\gamma-1}e^{-\alpha x^\gamma})\left((1+\beta)-2\beta\tan\left[\frac{\pi}{4}(1-e^{-\alpha x^\gamma})\right]\right)}{1-(1+\beta)\tan\left[\frac{\pi}{4}(1-e^{-\alpha x^\gamma})\right]+\beta\left(\tan\left[\frac{\pi}{4}(1-e^{-\alpha x^\gamma})\right]\right)^2}, \quad x>0, |\beta|\le 1, \alpha,\gamma>0. \tag{25}$$

The SF of the TTWD is obtained as

$$R(x) = 1-(1+\beta)\tan\left[\frac{\pi}{4}(1-e^{-\alpha x^\gamma})\right]+\beta\left(\tan\left[\frac{\pi}{4}(1-e^{-\alpha x^\gamma})\right]\right)^2, x>0, |\beta|\le 1, \alpha,\gamma>0. \tag{26}$$

The plot of the cdf of the TTWD is illustrated in Fig 2(a). The Fig.2(b) shows the pdf of the TTWD, which shows a decreasing and right-skewed trend. Moreover, the HF plots are shown in Fig.2(c), which shows increasing, decreasing, or unimodal bell-shaped curves, hence enhancing the distribution's adaptability to various lifetime data sets. Whereas the SF is decreasing for the given parameter values shown in Fig.2(d).

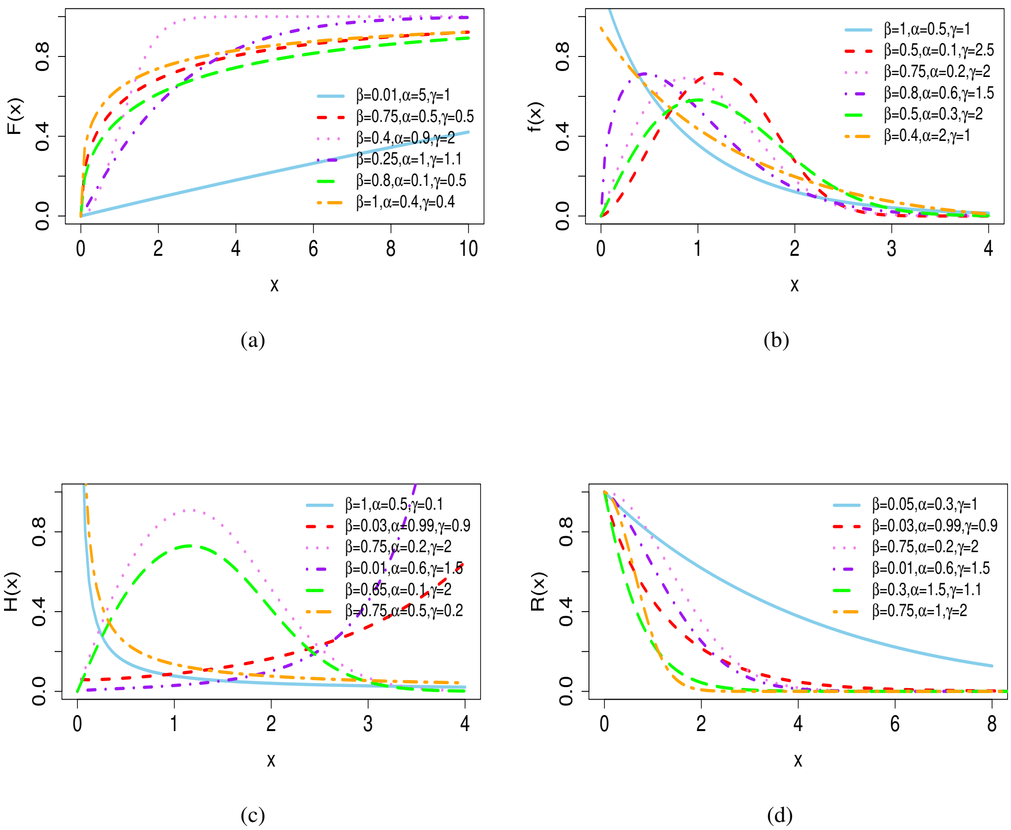

Figure 2. The cdf, pdf, HF and SF plots of the TTWD.

4.3. Transmuted tangent Rayleigh distribution

The cdf of the Rayleigh distribution is given by

$$G(x) = 1 - e^{-\alpha x^2}, \alpha > 0, x > 0. \tag{27}$$

The pdf of the Rayleigh distribution is given by

$$g(x) = 2\alpha x e^{-\alpha x^2}, \alpha > 0, x > 0. \tag{28}$$

The cdf of the transmuted tangent Rayleigh distribution (TTRD) is obtained as

$$F(x) = (1+\beta)\tan\left[\frac{\pi}{4}(1-e^{-\alpha x^2})\right] - \beta\left(\tan\left[\frac{\pi}{4}(1-e^{-\alpha x^2})\right]\right)^2, |\beta| \leq 1, x > 0 > 0. \tag{29}$$

The pdf of the TTRD is obtained as

$$f(x) = \frac{\pi}{4}\sec^2\left[\frac{\pi}{4}(1-e^{-\alpha x^2})\right](2\alpha x e^{-\alpha x^2})\left((1+\beta) - 2\beta\tan\left[\frac{\pi}{4}(1-e^{-\alpha x^2})\right]\right),$$
$$|\beta| \leq 1, x > 0 > 0. \tag{30}$$

The HF of the TTRD is obtained as

$$H(x) = \frac{\frac{\pi}{4}\sec^2\left[\frac{\pi}{4}(1-e^{-\alpha x^2})\right](2\alpha x e^{-\alpha x^2})\left((1+\beta)-2\beta\tan\left[\frac{\pi}{4}(1-e^{-\alpha x^2})\right]\right)}{1-(1+\beta)\tan\left[\frac{\pi}{4}(1-e^{-\alpha x^2})\right]+\beta\left(\tan\left[\frac{\pi}{4}(1-e^{-\alpha x^2})\right]\right)^2},$$
$$|\beta| \leq 1, x > 0, \alpha > 0. \tag{31}$$

The SF of the TTRD is obtained as

$$R(x) = 1-(1+\beta)\tan\left[\frac{\pi}{4}(1-e^{-\alpha x^2})\right]+\beta\left(\tan\left[\frac{\pi}{4}(1-e^{-\alpha x^2})\right]\right)^2, |\beta| \leq 1, x > 0, \alpha > 0. \tag{32}$$

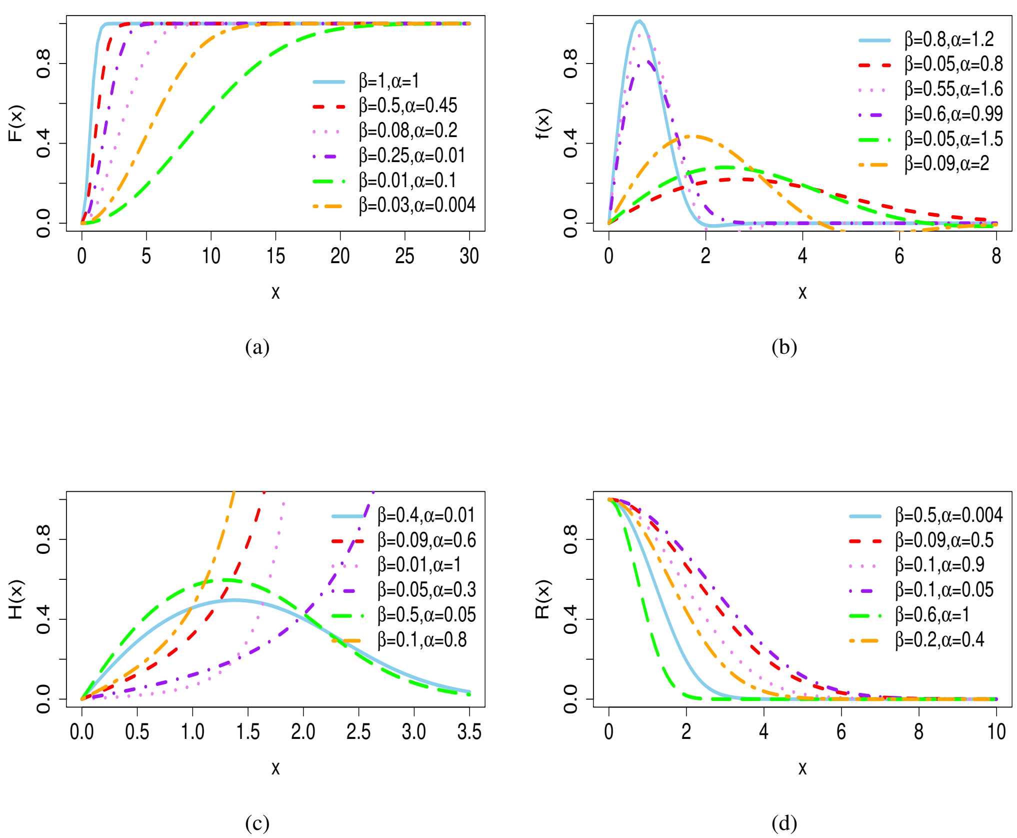

Figure 3. The cdf, pdf, HF and SF plots of the TTRD.

Fig. 3(a) shows the cdf of the TTRD. Fig.3(b) shows the pdf of the TTRD. The HF and SF of the TTRD are shown in Fig.3(c) and Fig.3(d), respectively.

4.4. Transmuted tangent Lindley distribution

The TTLD studied in detail in this section since the L distribution possesses good analytical ability.
The cdf of the L distribution is given by

$$G(x) = 1 - \frac{e^{-\alpha x}(\alpha x+\alpha+1)}{\alpha+1}, \alpha > 0, x > 0. \tag{33}$$

The pdf of the L distribution is given by

$$g(x) = \frac{\alpha^2}{(\alpha+1)}(x+1)e^{-\alpha x}, \alpha > 0, x > 0. \tag{34}$$

The cdf of the TTLD is obtained as

$$\begin{aligned} F(x) =&(1+\beta)\tan\left[\frac{\pi}{4}\left(1-\frac{e^{-\alpha x}(\alpha x+\alpha+1)}{\alpha+1}\right)\right]- \\ &\beta\left(\tan\left[\frac{\pi}{4}\left(1-\frac{e^{-\alpha x}(\alpha x+\alpha+1)}{\alpha+1}\right)\right]\right)^2, |\beta| \leq 1, \alpha > 0, x > 0. \end{aligned} \tag{35}$$

The pdf of the TTLD is obtained as

$$\begin{aligned} f(x) =&\frac{\pi}{4}\sec^2\left[\frac{\pi}{4}\left(1-\frac{e^{-\alpha x}(\alpha x+\alpha+1)}{\alpha+1}\right)\right]\left(\frac{\alpha^2}{(\alpha+1)}(x+1)e^{-\alpha x}\right) \\ &\times\left((1+\beta)-2\beta\tan\left[\frac{\pi}{4}\left(1-\frac{e^{-\alpha x}(\alpha x+\alpha+1)}{\alpha+1}\right)\right]\right), |\beta| \leq 1, \alpha > 0, x > 0. \end{aligned} \tag{36}$$

The HF of the TTLD is obtained as

$$\begin{aligned} H(x) =&\frac{\frac{\pi}{4}\sec^2\left[\frac{\pi}{4}\left(1-\frac{e^{-\alpha x}(\alpha x+\alpha+1)}{\alpha+1}\right)\right]\left(\frac{\alpha^2}{(\alpha+1)}(x+1)e^{-\alpha x}\right)\left((1+\beta)-2\beta\tan\left[\frac{\pi}{4}\left(1-\frac{e^{-\alpha x}(\alpha x+\alpha+1)}{\alpha+1}\right)\right]\right)}{1-\left[(1+\beta)\tan\left[\frac{\pi}{4}\left(1-\frac{e^{-\alpha x}(\alpha x+\alpha+1)}{\alpha+1}\right)\right]-\beta\left(\tan\left[\frac{\pi}{4}\left(1-\frac{e^{-\alpha x}(\alpha x+\alpha+1)}{\alpha+1}\right)\right]\right)^2\right]}, \\ &|\beta| \leq 1 \alpha > 0, x > 0. \end{aligned} \tag{37}$$

The SF of the TTLD is obtained as

$$\begin{aligned} R(x) =&1-\left[(1+\beta)\tan\left[\frac{\pi}{4}\left(1-\frac{e^{-\alpha x}(\alpha x+\alpha+1)}{\alpha+1}\right)\right]-\right. \\ &\left.\beta\left(\tan\left[\frac{\pi}{4}\left(1-\frac{e^{-\alpha x}(\alpha x+\alpha+1)}{\alpha+1}\right)\right]\right)^2\right], |\beta| \leq 1, \alpha > 0, x > 0. \end{aligned} \tag{38}$$

Fig. 4(a) shows the cdf of the TTLD for different parameter values. The pdf of the TTLD is shown in Fig.4(b) shows right-skewed and unimodal curves. The HF of the TTLD shows decreasing, increasing, J-shaped, and reverse J-shaped trends, as shown in Fig.4(c). The SF of the TTLD is shown in Fig.4(d).

4.4.1. Asymptotic property of the TTLD The asymptotic behaviour of the TTLD is given below

$$\begin{aligned} \lim_{x\to 0} f(x) &= \lim_{x\to 0}\frac{\pi}{4}\sec^2\left[\frac{\pi}{4}\left(1-\frac{e^{-\alpha x}(\alpha x+\alpha+1)}{\alpha+1}\right)\right]\left(\frac{\alpha^2}{(\alpha+1)}(x+1)e^{-\alpha x}\right) \\ &\times\left((1+\beta)-2\beta\tan\left[\frac{\pi}{4}\left(1-\frac{e^{-\alpha x}(\alpha x+\alpha+1)}{\alpha+1}\right)\right]\right) \\ &= \frac{\pi}{4}\lim_{x\to 0}\sec^2\left[\frac{\pi}{4}\left(1-\frac{e^{-\alpha x}(\alpha x+\alpha+1)}{\alpha+1}\right)\right] \\ &\times\frac{\alpha^2}{(\alpha+1)}\lim_{x\to 0}(x+1)e^{-\alpha x} \\ &\times\lim_{x\to 0}\left((1+\beta)-2\beta\tan\left[\frac{\pi}{4}\left(1-\frac{e^{-\alpha x}(\alpha x+\alpha+1)}{\alpha+1}\right)\right]\right) \\ &= \frac{\pi}{4}\frac{\alpha^2}{(\alpha+1)}(1+\beta). \end{aligned}$$

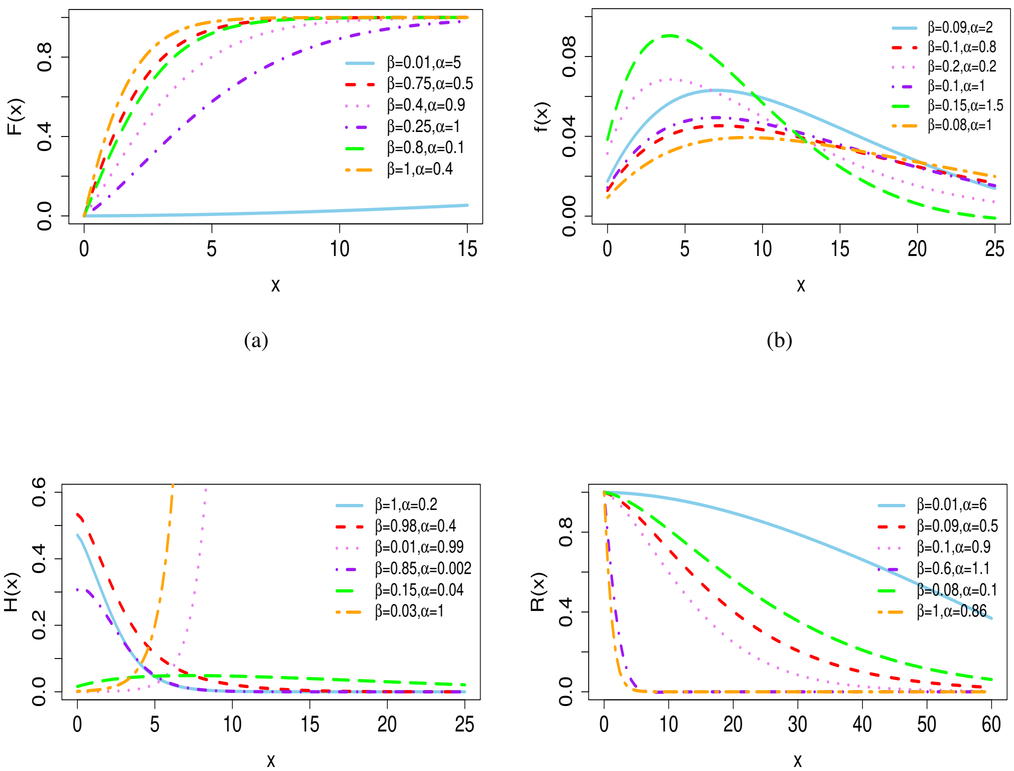

(a) (b) (c) (d)

Figure 4. The cdf, pdf, HF and SF plots of the TTLD.

$$
\begin{aligned}
\lim_{x\to\infty} f(x) &= \lim_{x\to\infty} \frac{\pi}{4}\sec^2\left[\frac{\pi}{4}\left(1-\frac{e^{-\alpha x}(\alpha x+\alpha+1)}{\alpha+1}\right)\right]\left(\frac{\alpha^2}{(\alpha+1)}(x+1)e^{-\alpha x}\right)\\
&\times\left((1+\beta)-2\beta\tan\left[\frac{\pi}{4}\left(1-\frac{e^{-\alpha x}(\alpha x+\alpha+1)}{\alpha+1}\right)\right]\right)\\
&= \frac{\pi}{4}\lim_{x\to\infty}\sec^2\left[\frac{\pi}{4}\left(1-\frac{e^{-\alpha x}(\alpha x+\alpha+1)}{\alpha+1}\right)\right]\\
&\times\frac{\alpha^2}{(\alpha+1)}\lim_{x\to\infty}(x+1)e^{-\alpha x}\\
&\times\lim_{x\to\infty}\left((1+\beta)-2\beta\tan\left[\frac{\pi}{4}\left(1-\frac{e^{-\alpha x}(\alpha x+\alpha+1)}{\alpha+1}\right)\right]\right)\\
&= 0.
\end{aligned}
$$

4.4.2. Order statistics of TTLD The order statistics of the TTLD is derived using the Eq.(11). The pdf of the i^{th} order statistics of the TTLD can be written as

$$f_i(x) = \left\{ \begin{array}{l} \dfrac{m!}{(i-1)!(m-i)!}\left[(1+\beta)\tan\left[\dfrac{\pi}{4}\left(1-\dfrac{e^{-\alpha x}(\alpha x+\alpha+1)}{\alpha+1}\right)\right]\right. \\ \left. -\beta\left(\tan\left[\dfrac{\pi}{4}\left(1-\dfrac{e^{-\alpha x}(\alpha x+\alpha+1)}{\alpha+1}\right)\right]\right)^2\right]^{i-1} \\ \times\left[1-(1+\beta)\tan\left[\dfrac{\pi}{4}\left(1-\dfrac{e^{-\alpha x}(\alpha x+\alpha+1)}{\alpha+1}\right)\right]\right. \\ \left. +\beta\left(\tan\left[\dfrac{\pi}{4}\left(1-\dfrac{e^{-\alpha x}(\alpha x+\alpha+1)}{\alpha+1}\right)\right]\right)^2\right]^{m-i} \\ \times\dfrac{\pi}{4}\sec^2\left[\dfrac{\pi}{4}\left(1-\dfrac{e^{-\alpha x}(\alpha x+\alpha+1)}{\alpha+1}\right)\right]\left(\dfrac{\alpha^2}{(\alpha+1)}(x+1)e^{-\alpha x}\right) \\ \times\left((1+\beta)-2\beta\tan\left[\dfrac{\pi}{4}\left(1-\dfrac{e^{-\alpha x}(\alpha x+\alpha+1)}{\alpha+1}\right)\right]\right), |\beta|\le 1, \alpha>0, x>0. \end{array} \right\} \tag{39}$$

The first-order statistic of the TTLD can be written as

$$f_1(x) = \left\{ \begin{array}{l} m\left[1-(1+\beta)\tan\left[\dfrac{\pi}{4}\left(1-\dfrac{e^{-\alpha x}(\alpha x+\alpha+1)}{\alpha+1}\right)\right]\right. \\ \left. +\beta\left(\tan\left[\dfrac{\pi}{4}\left(1-\dfrac{e^{-\alpha x}(\alpha x+\alpha+1)}{\alpha+1}\right)\right]\right)^2\right]^{m-1} \\ \times\dfrac{\pi}{4}\sec^2\left[\dfrac{\pi}{4}\left(1-\dfrac{e^{-\alpha x}(\alpha x+\alpha+1)}{\alpha+1}\right)\right]\times\left(\dfrac{\alpha^2}{(\alpha+1)}(x+1)e^{-\alpha x}\right) \\ \times\left((1+\beta)-2\beta\tan\left[\dfrac{\pi}{4}\left(1-\dfrac{e^{-\alpha x}(\alpha x+\alpha+1)}{\alpha+1}\right)\right]\right), |\beta|\le 1, \alpha>0, x>0. \end{array} \right\}$$

The m^{th} order statistics of the TTLD can be written as

$$f_m(x) = \left\{ \begin{array}{l} m\left[(1+\beta)\tan\left[\dfrac{\pi}{4}\left(1-\dfrac{e^{-\alpha x}(\alpha x+\alpha+1)}{\alpha+1}\right)\right]\right. \\ \left. -\beta\left(\tan\left[\dfrac{\pi}{4}\left(1-\dfrac{e^{-\alpha x}(\alpha x+\alpha+1)}{\alpha+1}\right)\right]\right)^2\right]^{m-1} \\ \times\dfrac{\pi}{4}\sec^2\left[\dfrac{\pi}{4}\left(1-\dfrac{e^{-\alpha x}(\alpha x+\alpha+1)}{\alpha+1}\right)\right]\left(\dfrac{\alpha^2}{(\alpha+1)}(x+1)e^{-\alpha x}\right) \\ \left((1+\beta)-2\beta\tan\left[\dfrac{\pi}{4}\left(1-\dfrac{e^{-\alpha x}(\alpha x+\alpha+1)}{\alpha+1}\right)\right]\right), |\beta|\le 1, \alpha>0, x>0. \end{array} \right\}$$

4.4.3. Quantile function of TTLD The random variable X from the TTLD and $p \in (0,1)$ then the quantile function can be derived as

$$Q_x(p) = -1-\frac{1}{\alpha}-\frac{1}{\alpha}W_{-1}\left[-e^{-(1+\alpha)}(\alpha+1)\left(1-\frac{4}{\pi}\arctan\left[\frac{(1+\beta)-\sqrt{(1+\beta)^2-4\beta p}}{2\beta}\right]\right)\right], \quad |\beta|\le 1, \alpha>0, x>0. \tag{40}$$

4.4.4. Parameter estimation In this section we are using three different methods for estimating the parameters of the TTLD.

Maximum likelihood estimation Consider $x_1, x_2, x_3, \cdots, x_n$ be n random samples from the TTLD. The log-likelihood function is $L = \sum_{i=1}^{n} \log f(x_i)$. The log-likelihood function of the TTLD is obtained as

$$L = \sum_{i=1}^{n} \log \left\{ \frac{\pi}{4} \sec^2 \left[\frac{\pi}{4} \left(1 - \frac{e^{-\alpha x_i}(\alpha x_i + \alpha + 1)}{\alpha + 1} \right) \right] \left(\frac{\alpha^2}{(\alpha+1)} (x_i + 1) e^{-\alpha x_i} \right) \times \left((1+\beta) - 2\beta \tan \left[\frac{\pi}{4} \left(1 - \frac{e^{-\alpha x_i}(\alpha x_i + \alpha + 1)}{\alpha + 1} \right) \right] \right) \right\}. \tag{41}$$

It can be simplified as

$$\begin{aligned} L =& n \log(\frac{\pi}{4}) + \sum_{i=1}^{n} \log(\sec^2 \left[\frac{\pi}{4} \left(1 - \frac{e^{-\alpha x_i}(\alpha x_i + \alpha + 1)}{\alpha + 1} \right) \right]) + n \log(\frac{\alpha^2}{\alpha+1}) + \sum_{i=1}^{n} \log(x_i + 1) \\ &- \alpha \sum_{i=1}^{n} x_i + \sum_{i=1}^{n} \log(\left((1+\beta) - 2\beta \tan \left[\frac{\pi}{4} \left(1 - \frac{e^{-\alpha x_i}(\alpha x_i + \alpha + 1)}{\alpha + 1} \right) \right] \right)). \end{aligned} \tag{42}$$

We derive the partial differential equation of Eq.(42) with respect to each parameter and equate it with zero, and it can be solved.
The partial differential equations are

$$\frac{\partial L}{\partial \beta} = \sum_{i=1}^{n} \frac{1 - 2\tan \left[\frac{\pi}{4} \left(1 - \frac{e^{-\alpha x_i}(\alpha x_i + \alpha + 1)}{\alpha + 1} \right) \right]}{(1+\beta) - 2\beta \tan \left[\frac{\pi}{4} \left(1 - \frac{e^{-\alpha x_i}(\alpha x_i + \alpha + 1)}{\alpha + 1} \right) \right]}. \tag{43}$$

$$\begin{aligned} \frac{\partial L}{\partial \alpha} =& -\frac{\pi}{2} \sum_{i=1}^{n} \tan \left[\frac{\pi}{4} \left(1 - \frac{e^{-\alpha x_i}(\alpha x_i + \alpha + 1)}{\alpha + 1} \right) \right] \times \\ & \frac{e^{-\alpha x_i} \left[-x_i(\alpha x_i + \alpha + 1)(\alpha + 1) + (x_i + 1)(\alpha + 1) - (\alpha x_i + \alpha + 1) \right]}{(\alpha+1)^2} \\ &+ \frac{2n}{\alpha} - \frac{n}{\alpha + 1} - \sum_{i=1}^{n} x_i + \sum_{i=1}^{n} \frac{\pi}{4} \frac{2\beta \sec^2 \left[\frac{\pi}{4} \left(1 - \frac{e^{-\alpha x_i}(\alpha x_i + \alpha + 1)}{\alpha + 1} \right) \right]}{(1+\beta) - 2\beta \tan \left[\frac{\pi}{4} \left(1 - \frac{e^{-\alpha x_i}(\alpha x_i + \alpha + 1)}{\alpha + 1} \right) \right]} \times \\ & \frac{e^{-\alpha x_i} \left[-x_i(\alpha x_i + \alpha + 1)(\alpha + 1) + (x_i + 1)(\alpha + 1) - (\alpha x_i + \alpha + 1) \right]}{(\alpha+1)^2}. \end{aligned} \tag{44}$$

Equations (43) and (44) can be solved to find the approximate solution for MLE of the TTLD.

Bayesian estimation The parameters of the TTLD are estimated by employing the Bayesian estimation method. We assume a gamma prior since the parameter α is greater than zero, and we choose a beta prior since the parameter β lies between [-1, 1]. Other appropriate distributions can also be used to choose priors. We employed the Markov Chain Monte Carlo (MCMC) approach to obtain samples from the posterior distribution of the parameters of the TTLD since the direct sampling is difficult. By the advantage of the Bayes theorem, the posterior distribution is defined as

$$f(\alpha, \beta | x, y) \propto f(y|x, \alpha, \beta) f(\alpha) f(\beta) = K f(y|x, \alpha, \beta) f(\alpha) f(\beta). \tag{45}$$

Where $f(y|x, \alpha, \beta)$ is the likelihood function of the TTLD, $f(\alpha)$ and $f(\beta)$ are the prior distributions for the parameters. The NO-U-Turn sampler (NUTS) is used to approximate the posterior distribution because it automatically tunes the step size, which makes it more robust.

Bayesian neural network The BNN uses steps similar to the classical Bayesian technique. As discussed in the Bayesian estimation method, the priors of the parameters are chosen similarly. That is $\alpha \sim \text{Gamma}(\omega_\alpha, \Omega_\alpha)$ since $\alpha > 0$ and $\beta \sim \text{Beta}(\omega_\beta, \Omega_\beta)$ since $\beta \in [-1, 1]$. The Bayes' theorem is applied to find the posterior distribution of the TTLD. The BNN is defined with three-layer feed forward propagation and activation function as ReLU function. The prior distributions are assigned as weights to deal with the uncertainty in their values. The Gamma prior is chosen with Gamma(2,1) and the Beta prior is chosen with Beta(2,2) as hyperparameters of the priors. We employed a feed-forward Bayesian neural network with an input layer with one feature, two hidden layers containing ten neurones each with ReLU activations, and an output layer with two outputs. Constraints were established by $\alpha = \text{softplus}(\alpha)$ (ensuring $\alpha > 0$) and $\beta = \tanh(\beta)$ (ensuring $-1 < \beta < 1$). We used the MCMC approach to obtain samples from the posterior distribution of the parameters of the TTLD. The posterior distribution of the network's weights and biases is estimated by MCMC sampling utilising the NUTS technique. It consists of 100 burn-in steps and 200 iterations; also, it runs a single MCMC chain. It converges with zero divergence It is not using point estimates (like gradient descent in a standard neural network). Instead, it samples from the posterior distribution over weights using Hamiltonian Monte Carlo (via NUTS). This gives a distribution over weights, not a single value.

Table 1. Simulation results for different parameter estimation methods.

Method=BNN					
Parameter	Sample Size	True value	Estimated value	Lower HDI	Upper HDI
α	100	1.1	1.1000774	1.0017266	1.1973284
	200	1.1	1.099689	0.99851996	1.1967367
	500	1.1	1.0998425	1.0007869	1.1965
	750	1.1	1.1000164	1.0007172	1.1978334
β	100	0.8	0.79995674	0.70210266	0.89807665
	200	0.8	0.80050534	0.7019766	0.8988638
	500	0.8	0.80011576	0.69955117	0.8967835
	750	0.8	0.800005	0.799303	0.800761
Method=Bayesian estimation					
Parameter	Sample Size	True value	Estimated value	Lower HDI	Upper HDI
α	100	1.1	1.051	0.876	1.248
	200	1.1	1.068	0.898	1.241
	500	1.1	1.101	0.940	1.278
	750	1.1	1.101	0.945	1.254
β	100	0.8	0.526	0.059	0.961
	200	0.8	0.618	0.253	0.966
	500	0.8	0.684	0.386	0.980
	750	0.8	0.709	0.425	0.979
Method=MLE					
Parameter	Sample Size	True value	Estimated value	Lower HDI	Upper HDI
α	100	1.1	1.48529	1.29600	1.89440
	200	1.1	1.15481	1.04317	1.30112
	500	1.1	1.56064	1.32707	1.75650
	750	1.1	1.27987	1.03987	1.56166
β	100	0.8	0.35075	-0.19492	0.58387
	200	0.8	0.60091	0.48116	0.74623
	500	0.8	-0.07692	-0.36634	0.30028
	750	0.8	0.41983	0.00977	0.82283

4.4.5. Simulation The simulation study is conducted to evaluate the effectiveness of the estimation methods. We have conducted the simulation studies for the different sample sizes, n=100,200,500,750 with 1000 replications and is presented in Table.1. For the parameter α for n=750 the MLE is 1.27987 and the actual value is 1.1 which

indicates the significant deviation from the actual value. From the table it is clear that the 95% highest density intervals (HDI) are (1.03987,1.56166) wider, and it suggests underestimation. The MLE for the parameter β at n=750, is 0.41983, the corresponding 95% HDIs are (0.00977, 0.82283). Which indicates wider HDIs.
For n=750 the Bayesian estimate of α is 1.101 and the corresponding 95%H DIs are (0.945,1.254). For the parameter β for n=750 the Bayesian estimate is 0.709 the corresponding 95% HDIs are (0.425, 0.979). It gives better results than MLE estimates.
From Table.1 the BNN estimate α is 1.1000164, it is very close to the actual value 1.1. Also the 95% HDIs are given by (1.0007172, 1.1978334). The interval reveals high accuracy in the estimates. The BNN estimate,β, for n=750, is 0.800005. The 95% HDI is (0.799303,0.800761). It also shows high confidence to the estimates. The simulation study is done using Python software in Google Colab which uses the libraries in Python, such as pyro, torch, numpy, PyMC3, etc. The BNN estimates show high precision compared to the MLE and Bayesian estimation methods even though it takes more running time. All the experiments were conducted in a machine which is configured with an 11th Gen Intel(R) Core(TM) i3-1115G processor and 8.00 GB RAM.

5. Data analysis

This section provides an application of the TTLD to cancer data sets. The data sets are selected from three different cancer types to show the flexibility of the family. The performance of the members of the TTFD is compared using the breast cancer data given in section 5.2; among them, the TTLD performs better with the low error measures and high p-value; hence, we choose the TTLD to compare with the other families of distributions. The results are given in table 2. We compare the efficiency of the TTFD through the TTLD with the other four well-established trigonometric families of distributions. Similar analysis can be done to TTED, TTWD, and TTRD belonging to

Table 2. MLEs and comparison criteria for the distributions in the TTFD.

Model	MLE	LL	AIC	BIC	HQIC	KS	p-value
TTLD	$\widehat{\alpha}$=0.04400757 $\widehat{\beta}$ = 0.33583595	580.252	1164.504	1170.096	1166.775	0.06364	0.7112
TTRD	$\widehat{\alpha}$=0.0003653551 $\widehat{\beta}$ = 0.5456991037	604.0176	1212.035	1217.627	1214.306	0.13861	0.03913
TTWD	$\widehat{\alpha}$=0.01899426 $\widehat{\beta}$ = 0.04559404 $\widehat{\gamma}$ = 1.08391557	581.1011	1168.202	1176.59	1171.609	0.10492	0.5393
TTED	$\widehat{\alpha}$=0.03559367 $\widehat{\beta}$=-0.40630820	581.3904	1166.781	1172.372	1169.052	0.12555	0.6441

the TTFD. The comparison of TTLD with existing distribution:

- Hyperbolic tangent inverse exponential distribution (HTIE)[26]

$$F(x) = \left(\frac{e^a + e^{-a}}{e^a - e^{-a}}\right)\tanh(ae^{\frac{-\theta}{x}}); x > 0, \theta > 0, a > 0.$$

- Hyperbolic cosine exponential distribution (HCE)[15]

$$F(x) = \frac{2e^a}{e^{2a} - 1}\sinh(a(1 - e^{-\lambda x})), \lambda > 0, a > 0, x > 0.$$

- New hyperbolic sine Rayleigh distribution (NHSRD)[1]

$$F(x) = \frac{2e^{(1-a)}}{(e^{(1-a)} - 1)^2}(\cosh(a^{1-e^{-\theta x^2}} - 1) - 1), x > 0, \theta > 0, a > 0.$$

- Cosine Weibull distribution (CosW)[39]

$$F(x) = 1 - \sin\left(\frac{\pi}{2}(exp(-(\lambda x)^{\alpha}))\right), \lambda > 0, a > 0, x > 0.$$

We employ various discriminative measures, including the Bayesian Information Criterion (BIC), Akaike Information Criterion (AIC) and Hannan-Quinn Information Criterion (HQIC) to assess the adaptability of the TTLD. A distribution with lower BIC, AIC, and HQIC values is considered a superior fit. Furthermore, we utilise the Kolmogorov-Smirnov test statistic (KS), LL function, and p-value. A high p-value and lower LL and KS values imply a superior fit to the data. Ultimately, we present the histograms of the data sets and illustrate the fitted density functions to facilitate a visual comparison of the families. The descriptive measures of the data sets are given in Table 3.

5.1. *Head and Neck cancer data*

This data set illustrates the survival times of patients with head and neck cancer. The patients received treatment through radiotherapy and chemotherapy. It was previously studied by Efron [7]. The hazard rate of the data was measured using the total time on test transform (TTT) plot given in 5(b).
Data set I: 12.2, 23.56, 23.74, 25.87, 31.98, 37, 41.35, 47.38, 55.46,58.36, 63.47, 68.46, 78.26, 74.47, 81.43, 84, 92, 94,110, 112, 119,127, 130, 133, 140, 146, 155,159 ,173 ,179, 194, 195, 209, 249, 281, 319,339, 432, 469, 519, 633, 725, 817, 1776.

Table 3. Descriptive measures of data sets

	n	Mean	Median	Mode	Min	Max	Variance	Skewness	Kurtosis
Data set I	44	223.477	128.5	100	12.2	1776	93286.41	3.38382	13.5596
Data set II	121	46.32893	40	10	0.3	154	1244.464	1.04318	0.40214
Data set III	42	12.88095	10.5	6,8	1	35	87.37573	0.87599	-0.12996

Table 4. MLEs and comparison criteria for data set I

Model	MLE	LL	AIC	BIC	HQIC	KS	p-value
TTLD	$\widehat{\alpha} = 0.01114032$	292.0735	588.1469	591.7153	589.4703	0.9344803	0.4909
	$\widehat{\beta} = 0.51419030$						
HTIE	$\widehat{a}$=0.9711573	406.7488	817.4976	821.066	818.821	0.48284	5.789e-10
	$\widehat{\theta}$ = 4.7218041						
HCE	$\widehat{a}$=4.85365979	394.5152	793.0304	796.5987	794.3537	0.40768	4.002e-07
	$\widehat{\lambda}$=0.02888578						
NHSRD	$\widehat{a}$=1.689926	539.4779	1082.956	1086.524	1084.279	0.31322	0.0002466
	$\widehat{\theta}$=5.319295e-05						
CosW	$\widehat{\alpha}$ = 0.2328192	315.4279	634.8559	638.4243	636.1792	0.53207	3.711e-12
	$\widehat{\lambda}$=0.1015042						

5.2. *Breast cancer data*

This dataset illustrates the survival times of 121 breast cancer patients sourced from a major hospital between 1929 and 1938, as documented by Lee [18]. The hazard shape of the data measured using the TTT plot is given in 6(b).
Data set II: 0.3, 4.0, 0.3, 5.0, 6.2, 5.6, 6.3, 6.8, 6.6, 7.4, 8.4, 7.5, 8.4, 11.0, 10.3, 11.8, 12.3, 12.2, 14.4, 13.5, 14.8, 14.4, 15.5, 16.2, 15.7, 16.3, 16.8, 16.5, 17.2, 17.5, 17.3, 17.9, 20.4, 19.8, 20.9, 21.0, 21.0, 21.1, 23.4, 23.0, 23.6, 27.9, 24.0, 28.2, 24.0, 29.1, 31.0, 30.0, 31.0, 35.0, 32.0, 37.0, 35.0, 37.0, 38.0,37.0, 38.0, 45.0,39.0, 41.0, 39.0,

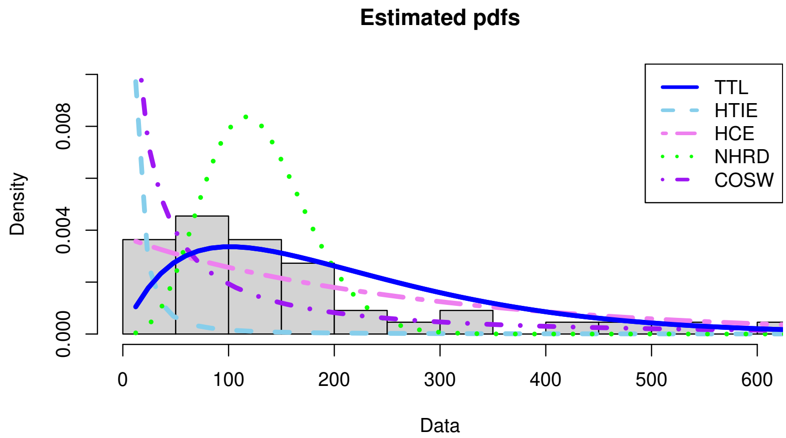

(a)

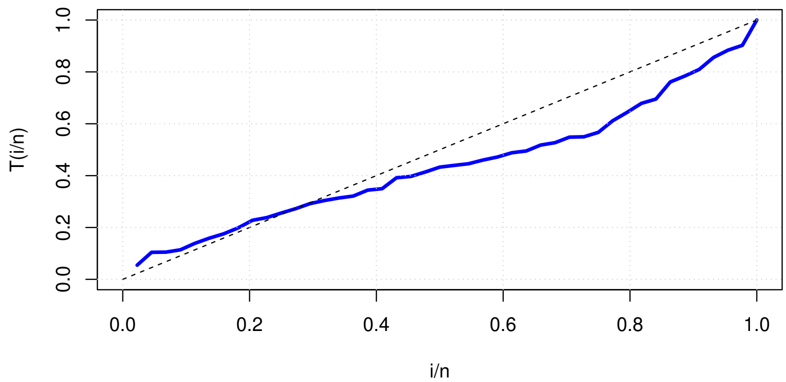

(b)

Figure 5. The pdf plots and TTT plot of data set I

40.0, 38.0, 40.0, 43.0, 41.0, 43.0, 41.0, 40.0, 42.0, 44.0, 43.0, 45.0, 48.0, 46.0, 47.0, 46.0, 51.0, 49.0, 51.0, 52.0, 51.0, 55.0, 54.0, 56.0, 58.0, 57.0, 59.0, 62.0, 60.0, 65.0, 60.0, 67.0, 60.0, 61.0, 65.0, 68.0,67.0, 69.0, 80.0, 78.0, 83.0, 89.0, 88.0, 90.0, 96.0, 93.0, 105.0, 103.0, 109.0, 111.0, 109.0, 115.0, 125.0, 117.0, 126.0, 129.0, 129.0, 154.0, 127.0, 139.0.

5.3. Leukemia data

The remission periods of individuals with acute leukaemia were analysed to evaluate the efficacy of 6-MP in maintaining remission time. This data was previously used by Freireich et al. [9]. The hazard shape of the data illustrated using the TTT plot is given in 7(b).
Data set III: 6, 6, 6, 7, 10, 13, 16, 22, 23, 6, 9, 10, 11, 17, 19, 20, 25, 32, 32, 34, 35, 1, 1, 2, 2, 3, 4, 4, 5, 5, 8, 8, 8, 8, 11, 11, 12, 12, 15, 17,22, 23.

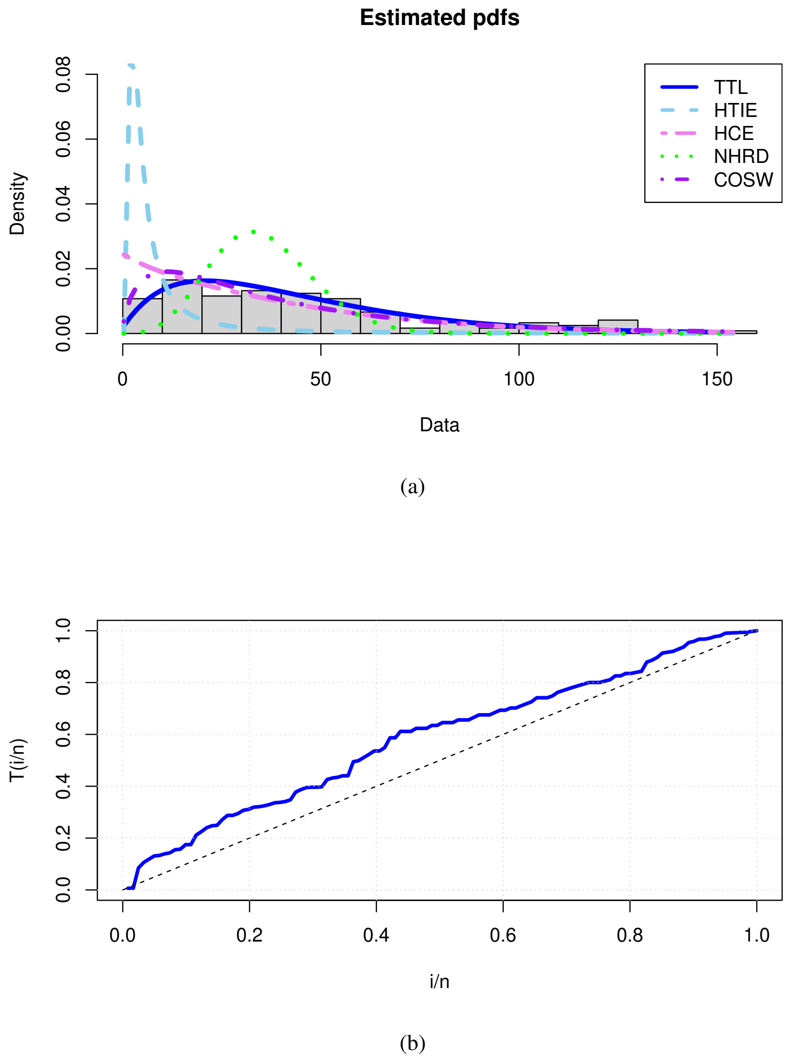

Figure 6. The pdf plots and TTT plot of data set II

6. Results

Table 1 shows that as n increases, the BNN method gives a better approximation to the true value of the parameters as compared to the Bayesian estimation and MLE method. The Bayesian method perform better as compared to the MLE method as it gives closer values to the true values of the parameters.

Three cancer datasets regarding the remission periods or survival times of different cancer patients were utilised to evaluate the suitableness of the TTFD in comparison to other established families. The efficiency of the suggested family is evaluated by the use of goodness-of-fit measures. Tables 4-6 demonstrate that the suggested family surpasses the other four families, offering a superior fit for the data set as indicated by the highest p-value of the K-S statistics. The TTLD gives the lowest AIC, BIC, and HQIC to the data sets as compared with its competitors. The lowest values of the error measures also indicate a good fit to the data sets. Consequently, the TTFD is appropriate, as it fits more effectively with the datasets compared to alternative families. Moreover, a comparison of the pdfs with the calculated parameter values reveals the optimal fit illustrated in Fig. 5(a), Fig. 6(a) and Fig.7(a).

Table 5. MLEs and comparison criteria for data set II

Model	MLE	LL	AIC	BIC	HQIC	KS	p-value
TTLD	$\widehat{\alpha}$=0.04400757	580.252	1164.504	1170.096	1166.775	0.06364	0.7112
	$\widehat{\beta}$ = 0.33583595						
HTIE	$\widehat{a}$=0.9597745	809.8344	1623.669	1629.26	1625.94	0.44233	2.2e-16
	$\widehat{\theta}$ = 4.9854785						
HCE	$\widehat{a}$=1.58115998	582.6202	1169.24	1174.832	1171.511	0.13534	0.02376
	$\widehat{\lambda}$=0.03147176						
NHSRD	$\widehat{a}$=1.318810567	766.4766	1536.953	1542.545	1539.224	0.2122	3.702e-05
	$\widehat{\theta}$=0.001002918						
CosW	$\widehat{\alpha}$ =0.46099355	620.8464	1245.693	1251.284	1247.964	0.30945	1.725e-10
	$\widehat{\lambda}$ =0.07349516						

Table 6. MLEs and comparison criteria for data set III

Model	MLE	LL	AIC	BIC	HQIC	KS	p-value
TTLD	$\widehat{\alpha}$ = 0.1567516	146.1109	296.2218	299.6972	297.4957	0.068944	0.9884
	$\widehat{\beta}$ = 0.1636023						
HTIE	$\widehat{a}$=1.470990	177.9557	359.9113	363.3867	361.1852	0.29527	0.00132
	$\widehat{\theta}$ = 4.893578						
HCE	$\widehat{a}$ = 3.0169966	147.1796	298.3591	301.8345	299.633	0.13776	0.4028
	$\widehat{\lambda}$=0.1189993						
NHSRD	$\widehat{a}$=1.133070571	176.4619	356.9238	360.3992	358.1977	0.33691	0.0001446
	$\widehat{\theta}$=0.005942723						
CosW	$\widehat{\alpha}$ =0.9365613	149.5708	303.1416	306.6169	304.4154	0.20282	0.06315
	$\widehat{\lambda}$=0.1492574						

Furthermore, the TTT plot indicates the characteristics of the HF of the given data. The curve is initially concave and subsequently convex in Fig.5(b), indicating that the HF is unimodal. In Fig.6(b) and Fig.7(b), the curve is concave, indicating that the HF is increasing. Consequently, we assert that the suggested family is effective for estimating the survival and remission times in cancer datasets.

7. Conclusion

Cancer is one of the crucial contributors to the immature mortality rate. It is important to study and analyse the remission periods or survival times of cancer patients with the help of probability distributions. Classical distributions may inadequately represent the datasets. The TTFD is introduced to make more flexible distributions for better modelling of the lifetime data sets. Various structural properties are examined, including SF, HF, reverse hazard function, ordinary and incomplete moments, quantile function, order statistics, etc. We generated four special members from TTFD, such as TTED, TTWD, TTRD, and TTLD; their pdf, cdf, HF, and SF are also derived and illustrated graphically. We have estimated the parameters of the TTLD using three different methods such that BNN, Bayesian estimation and MLE. This study indicates that the BNN estimation gives accurate results compared to the other two. We used three sets of remission periods or survival times of cancer data sets to emphasise the potentiality of this novel family. We executed data analysis using TTLD. The TTLD provides a superior fit compared to other competing distributions derived from established families. We anticipate that this generalisation will garner broader applicability across other domains.

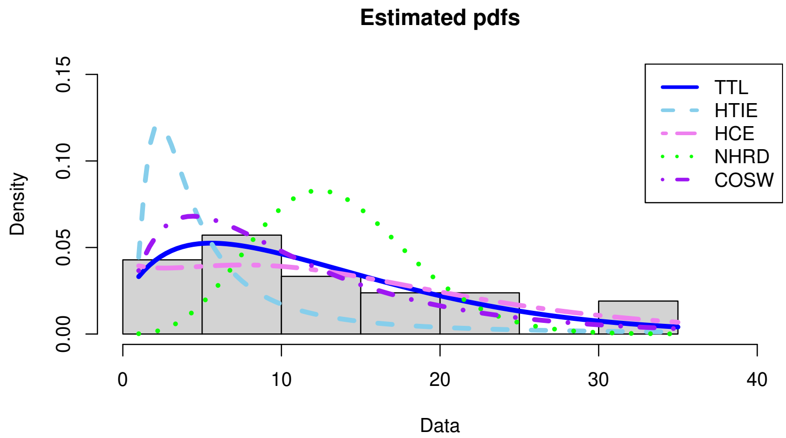

(a)

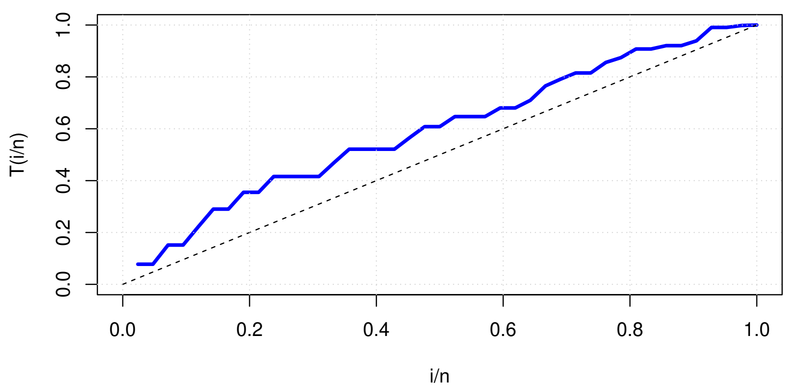

(b)

Figure 7. The pdf plots and TTT plot of data set III

Data availability statement

The authors confirm that the data supporting the findings of this study are available within the article.

Author Contributions

All the authors contributed equally to the completion of this manuscript. The manuscript has been revised, analysed, and approved by the authors.

REFERENCES

1. A. Ahmad, N. Alsadat, M. N. Atchade, S. Q. ul Ain, A. M. Gemeay, M. A. Meraou, E. M. Almetwally, M. M. Hossain, and E. Hussam, *New hyperbolic sine-generator with an example of Rayleigh distribution: Simulation and data analysis in industry*, Alexandria Engineering Journal, vol. 73, no. 1, pp. 415–426, 2023.
2. M. Ahsanullah, *Record Values: Theory, Methods and Applications*, University Press of America, Inc., New York, 2004.
3. N. Alsadat, C. Taniş, L. P. Sapkota, C. S. Rajitha, M. M. Bahloul, and A. M. Gemeay, *Power unit exponential probability distribution: Statistical inference and applications*, Alexandria Engineering Journal, vol. 107, pp. 332–346, 2024.
4. A. Alzaatreh, C. Lee, and F. Famoye, *A new method for generating families of continuous distributions*, Metron, vol. 71, no. 1, pp. 63–79, 2013.
5. C. B. Ampadu, *The hyperbolic Tan-X family of distributions: Properties, application and characterization*, Journal of Statistical Modelling: Theory and Applications, vol. 2, no. 1, pp. 1–13, 2021.
6. L. Bortolussi, G. Carbone, L. Laurenti, A. Patane, G. Sanguinetti, and M. Wicker, *On the robustness of Bayesian neural networks to adversarial attacks*, IEEE Transactions on Neural Networks and Learning Systems, vol. 36, no. 4, pp. 6679–6692, 2024.
7. B. Efron, *Logistic regression, survival analysis, and the Kaplan-Meier curve*, Journal of the American Statistical Association, vol. 83, no. 402, pp. 414–425, 1988.
8. F. Y. Eissa, C. D. Sonar, O. A. Alamri, and A. H. Tolba, *Statistical inferences about parameters of the pseudo Lindley distribution with acceptance sampling plans*, Axioms, vol. 13, no. 7, pp. 443, 2024.
9. E. Freireich, E. Gehan, E. Frei III, L. R. Schroeder, I. J. Wolman, R. Anbri, E. O. Burgert, S. D. Mills, D. Tinkel, O. S. Selawry, *et al.*, *The effect of 6-mercaptopurine on the duration of steroid-induced remissions in acute leukemia: A model for evaluation of other potentially useful therapy*, Blood, vol. 21, pp. 699–716, 1963.
10. R. C. S. Guptha and S. K. Maruthan, *A new generalization of power Lindley distribution and its applications*, Thailand Statistician, vol. 21, no. 1, pp. 196–208, 2023.
11. A. S. Hassan and S. G. Nassr, *Power Lindley-G family of distributions*, Annals of Data Science, vol. 6, pp. 189–210, 2019.
12. A. S. Hassan, D. S. Metwally, M. Elgarhy, H. E. Semary, A. Faal, and R. E. Mohamed, *Sine Power Unit Inverse Lindley Model: Bayesian Analysis and Practical Application*, Engineering Reports, vol. 7, no. 6, pp. e70242, 2025.
13. G. H. Jowett, *The exponential distribution and its applications*, The Incorporated Statistician, vol. 8, no. 2, pp. 89–95, 1958.
14. K. Karakaya, C. S. Rajitha, Ş. Sağlam, Y. A. Tashkandy, M. E. Bakr, A. H. Muse, A. Kumar, E. Hussam, and A. M. Gemeay, *A new unit distribution: Properties, estimation, and regression analysis*, Scientific Reports, vol. 14, no. 1, p. 7214, 2024.
15. O. Kharazmi and A. Saadatinik, *Hyperbolic cosine-F family of distributions with an application to exponential distribution*, Gazi University Journal of Science, vol. 29, no. 4, pp. 811–829, 2016.
16. O. Kharazmi, A. Saadatinik, M. Alizadeh, and G. G. Hamedani, *Odd hyperbolic cosine-FG family of lifetime distributions*, Journal of Statistical Theory and Applications, vol. 18, no. 4, pp. 387–401, 2019.
17. A. Kumari, I. Ghosh, and K. Kumar, *Bayesian and likelihood estimation of multicomponent stress–strength reliability from power Lindley distribution based on progressively censored samples*, Journal of Statistical Computation and Simulation, vol. 94, no. 5, pp. 923–964, 2024.
18. E. T. Lee, *Statistical Methods for Survival Data Analysis*, IEEE Transactions on Reliability, vol. 35, no. 1, p. 123, 1986.
19. D. V. Lindley, *Fiducial distributions and Bayes' theorem*, Journal of the Royal Statistical Society, Series B (Methodological), vol. 20, no. 1, pp. 102–107, 1958.
20. M. Magris and A. Iosifidis, *Bayesian learning for neural networks: an algorithmic survey*, Artificial Intelligence Review, vol. 56, no. 10, pp. 11773–11823, 2023.
21. A. Mahdavi, *Generalized Topp-Leone family of distributions*, Journal of Biostatistics and Epidemiology, vol. 3, no. 2, pp. 65–75, 2017.
22. Z. Mahmood, C. Chesneau, and M. H. Tahir, *A new sine-G family of distributions: Properties and applications*, Bulletin of Computational Applied Mathematics, vol. 7, no. 1, pp. 53–81, 2019.
23. I. Makhdoom, S. Y. Shahrastani, and F. G. Sharifonnasabi, *Bayesian Inference for the Lindley Distribution under Type-II Censoring with Fuzzy Data*, Journal of Data Science and Modeling, pp. 245–265, 2025.
24. A. W. Marshall and I. Olkin, *A new method for adding a parameter to a family of distributions with application to the exponential and Weibull families*, Biometrika, vol. 84, no. 3, pp. 641–652, 1997.
25. P. Marthin and G. S. Rao, *Transmuted Generalized Weibull Lindley (TGWL) distribution: Bayesian inference and Bayesian neural network approaches for lifetime data modeling*, Heliyon, vol. 11, no. 5, 2025.
26. S. Mohammad and I. Mendoza, *A new hyperbolic tangent family of distributions: Properties and applications*, Annals of Data Science, vol. 11, no. 1, pp. 1–24, 2024.
27. M. Nagy, A. M. Gemeay, C. S. Rajitha, K. Karakaya, Ş. Sağlam, A. H. Mansi, and M. Kilai, *Power unit Gumbel type II distribution: Statistical properties, regression analysis, and applications*, AIP Advances, vol. 13, no. 11, 2023.
28. R. M. Neal, *Bayesian learning for neural networks*, Springer Science & Business Media, vol. 118, 2012.
29. C. S. Rajitha and A. Akhilnath, *Generalization of the Lindley distribution with application to COVID-19 data*, International Journal of Data Science and Analytics, pp. 1–21, 2022.
30. C. S. Rajitha and K. Anisha, *The odd Weibull Lindley distribution for modeling wind energy data*, International Journal of Data Science and Analytics, vol. 17, no. 1, pp. 1–24, 2024.
31. C. S. Rajitha and R. Ashly, *The negative binomial-Akash distribution and its applications*, Reliability: Theory & Applications, vol. 17, no. 2 (68), pp. 482–491, 2022.
32. C. S. Rajitha and M. Vaishnavi, *Power exponentiated Weibull distribution: Application in survival rate of cancer patients*, Lobachevskii Journal of Mathematics, vol. 44, no. 9, pp. 3806–3824, 2023.
33. RStudio Team, *RStudio: Integrated Development Environment for R*, RStudio, PBC, Boston, MA, 2020. Available: http://www.rstudio.com/

34. K. M. Sakthivel and J. Rajkumar, *Transmuted sine-G family of distributions: Theory and applications*, Statistics and Applications, vol. 20, no. 2, pp. 73–92, 2021.
35. K. M. Sakthivel, C. S. Rajitha, and K. Dhivakar, *Two parameter cubic rank transmutation of Lindley distribution*, AIP Conference Proceedings, vol. 2261, no. 1, 2020.
36. W. T. Shaw and I. R. C. Buckley, *The alchemy of probability distributions: Beyond Gram-Charlier expansions, and a skew-kurtotic-normal distribution from a rank transmutation map*, arXiv preprint, arXiv:0901.0434, 2007.
37. I. Soerjomataram and F. Bray, *Planning for tomorrow: Global cancer incidence and the role of prevention 2020–2070*, Nature Reviews Clinical Oncology, vol. 18, no. 10, pp. 663–672, 2021.
38. L. Souza, W. Junior, C. De Brito, C. Chesneau, T. Ferreira, and L. Soares, *On the Sin-G class of distributions: Theory, model and application*, Journal of Mathematical Modeling, vol. 7, no. 3, pp. 357–379, 2019.
39. L. Souza, W. R. de O. Júnior, C. C. R. de Brito, T. A. E. Ferreira, and L. G. M. Soares, *General properties for the Cos-G class of distributions with applications*, Eurasian Bulletin of Mathematics, vol. 2, no. 2, pp. 63–79, 2019.
40. L. Souza, W. R. de O. Júnior, C. C. R. de Brito, C. Chesneau, R. L. Fernandes, and T. A. E. Ferreira, *Tan-G class of trigonometric distributions and its applications*, Cubo (Temuco), vol. 23, no. 1, pp. 1–20, 2021.
41. W. Yin, W. Yang, and H. Liu, *A neural network scheme for recovering scattering obstacles with limited phaseless far-field data*, Journal of Computational Physics, vol. 417, p. 109594, 2020.